

1  
2  
3  
4  
5  
6  
7  
8  
9  
10  
11  
12  
13  
14  
15  
16  
17  
18  
19  
20  
21  
22  
23  
24  
25  
26  
27  
28  
29  
30  
31  
32  
33  
34  
35  
36  
37

*Paleoceanography and Paleoclimatology*

Supporting Information for

**Drivers of late Miocene tropical sea surface cooling: a new perspective from the equatorial Indian Ocean**

Claire Martinot<sup>1\*</sup>, Clara T. Bolton<sup>1\*</sup>, Anta-Clarisse Sarr<sup>1</sup>, Yannick Donnadieu<sup>1</sup>, Marta Garcia<sup>1</sup>,  
Emmeline Gray<sup>1,2</sup>, Kazuyo Tachikawa<sup>1</sup>

1. Aix Marseille Univ, CNRS, IRD, INRAE, Coll France, CEREGE, Aix-en-Provence, France

2. Now at: School of Environment, Earth and Ecosystem Sciences, The Open University, Milton Keynes, UK

**Contents of this file**

Texts S1 to S4  
Figures S1 to S9

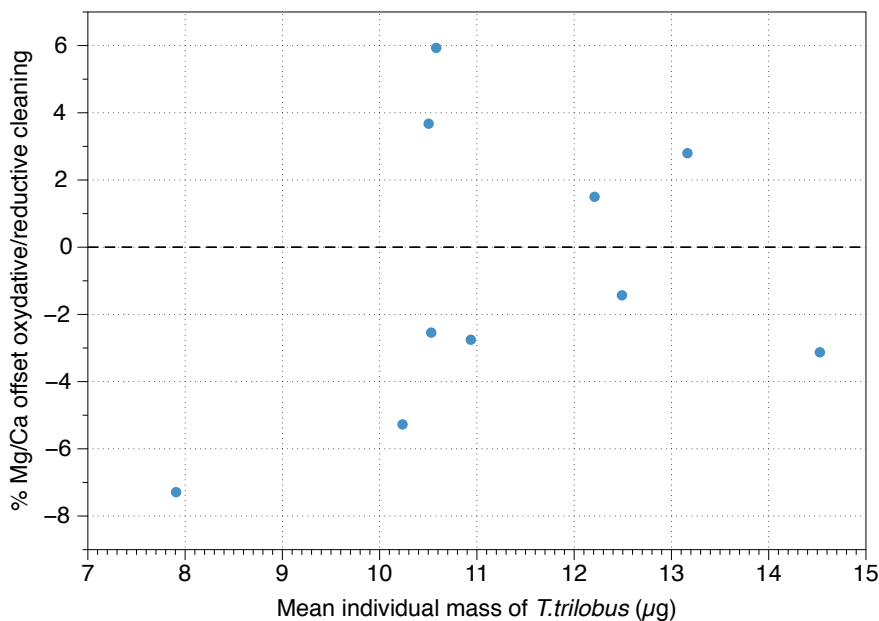
**Introduction**

Supplemental Texts and Figures S1 to S5 provide more detailed information about the methods used to reconstruct SST from Mg/Ca. Texts S1 and S2 and Figures S1 and S2 assess Mg/Ca ratio sensitivity to cleaning method and foraminiferal test size. Texts S3 and S4 and Figures S3 to S5 describe and compare the effect of different calibrations, scenarios for seawater Mg/Ca variations, and associated corrections on reconstructed SST.

Supplemental Figures S6 to S9 provide further context to Mg/Ca-SST data presented in the main text. Figure S6 shows indicators of cleaning performance and test dissolution together with SEM images. Figure S7 compares time series analyses of Mg/Ca-SST record from Site U1443 (South Bay of Bengal) to the other existing tropical high-resolution Mg/Ca-SST records from Site 1146 (South China Sea) spanning the time interval from ~8 to 5 Ma. Figure S8 shows long term trends of other existing tropical low resolution SST records based on the  $TEX_{86}$  and  $U^{K'}_{37}$  indices. Figure S9 is a map showing the effect of  $pCO_2$  variations on modelled SSTs in tropical Indian Ocean during the late Miocene.

38 **Text S1. Sensitivity of Mg/Ca<sub>foram</sub> to cleaning protocol**

39 In our samples from Site U1443, test fragments of *T. trilobus* for Mg/Ca analysis were  
40 cleaned to remove clay and organic matter, following the « Mg » protocol from Barker et al.  
41 (2003) without a reductive step (oxidative cleaning) whereas Dekens et al. (2002) used a « Cd »  
42 cleaning protocol from Boyle & Keigwin (1985) and Mashiotta et al. (1999) including a reductive  
43 step. It was reported that the « Cd » cleaning protocol often results in a lowering of the Mg/Ca  
44 ratio of 8 % compared to the « Mg » protocol by preferential dissolution of the Mg-rich parts of  
45 the test (Rosenthal et al. 2004). In order to confidently apply the Dekens et al. (2002) calibration,  
46 we tested the sensitivity of Mg/Ca to reductive cleaning in ten samples covering our late Miocene  
47 study interval. The samples were split after homogenization of crushed tests and one half was  
48 cleaned following the « Mg » protocol and the other half was cleaned following the « Cd »  
49 protocol. As observed in Figure S1, the difference in cleaning protocol does not result in a  
50 constant Mg/Ca offset, and there is no clear trend between the offset between the two cleaning  
51 protocol and the mean individual mass of *T. trilobus* tests. Therefore, we did not apply a  
52 correction to raw Mg/Ca ratios to account for the difference in cleaning protocol.  
53



54  
55

56 **Figure S1. Cleaning protocol sensitivity test.**

57 The % Mg/Ca offset between oxidative and reductive cleaning versus the mean individual mass  
58 of *T. trilobus* tests (total mass before crushing/number of individuals in population).

59 **Text S2. Sensitivity of Mg/Ca<sub>foram</sub> to test size**

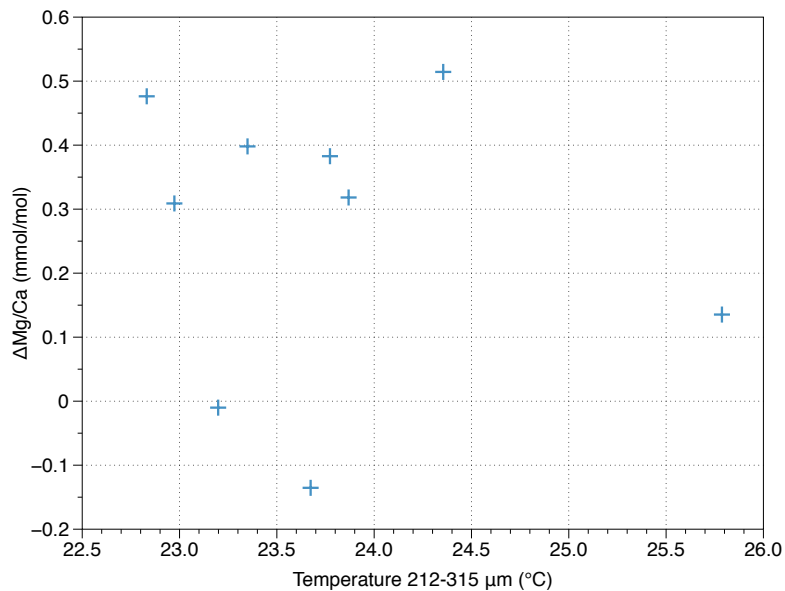
60 A test to determine Mg/Ca sensitivity to *T. trilobus* test size was performed for nine samples in  
61 two size fractions: 212-315 µm and 355-500 µm. The  $\Delta$ Mg/Ca (Mg/Ca 355-500 µm – Mg/Ca  
62 212-315 µm) is represented as a function of the temperature calculated from Mg/Ca ratios in the  
63 212-315 µm size fraction by applying the calibration of Anand et al. (2003). No correlation is  
64 observed between changes in  $\Delta$ Mg/Ca and temperature (Figure S2). For 7 of the 9 samples,  
65 Mg/Ca ratio increases with test size. For 6 samples the  $\Delta$ Mg/Ca is relatively constant: the tests  
66 from the 350-500 µm size fraction have a Mg/Ca ratio ~0.4 mmol/mol higher than the Mg/Ca of  
67 the smaller foraminifera (212-315 µm), representing an average variation of 13.8 % of the Mg/Ca  
68 ratio. However, for three of the samples this variation is not observed; for one sample the

69  $\Delta\text{Mg}/\text{Ca}$  is 0.15 mmol/mol, for another sample it is negligible and for the last one it is negative.  
70 Therefore, the  $\Delta\text{Mg}/\text{Ca}$  is not constant over our whole record.

71 It should be noted that previous work that has investigated the relationship between Mg/Ca ratio  
72 and the size of foraminiferal tests shows contradictory trends. Elderfield et al. (2002) and Drury et  
73 al., (2018) observe a positive correlation (Mg/Ca ratio increases with test size). Elderfield et al.  
74 (2002) suggest that the signal would reflect a change in calcification rate, with smaller individuals  
75 calcifying faster and larger individuals forming calcite more in equilibrium with seawater  
76 composition. On the contrary, the general trend observed by Friedrich et al. (2012) is a negative  
77 correlation (Mg/Ca ratio decreases with test size); these authors interpret this signal as mainly  
78 environmentally controlled, and suggest it reflects a change in the habitat of foraminifera during  
79 their life cycle, with larger individuals migrating deeper in the water column. As in most of our  
80 selected samples, Mg/Ca and size test show a positive correlation, and foraminifera in the two  
81 size fractions were selected to exclude mature individuals with gametogenic calcite known to  
82 migrate deeper in the water column before reproduction, the second hypothesis from Friedrich et  
83 al. (2012) for our data is more unlikely.

84 However, because the observed positive correlation is not constant in all the samples, the same  
85 correction for our entire record is difficult to envisage, the decision was made to not apply a  
86 "size" correction to Mg/Ca values to compensate for the difference in size between our samples  
87 and those of certain calibrations (Anand et al., 2003), but rather to apply the calibration from  
88 Dekens et al. (2002) using a similar size fraction (250-355  $\mu\text{m}$ ).

89

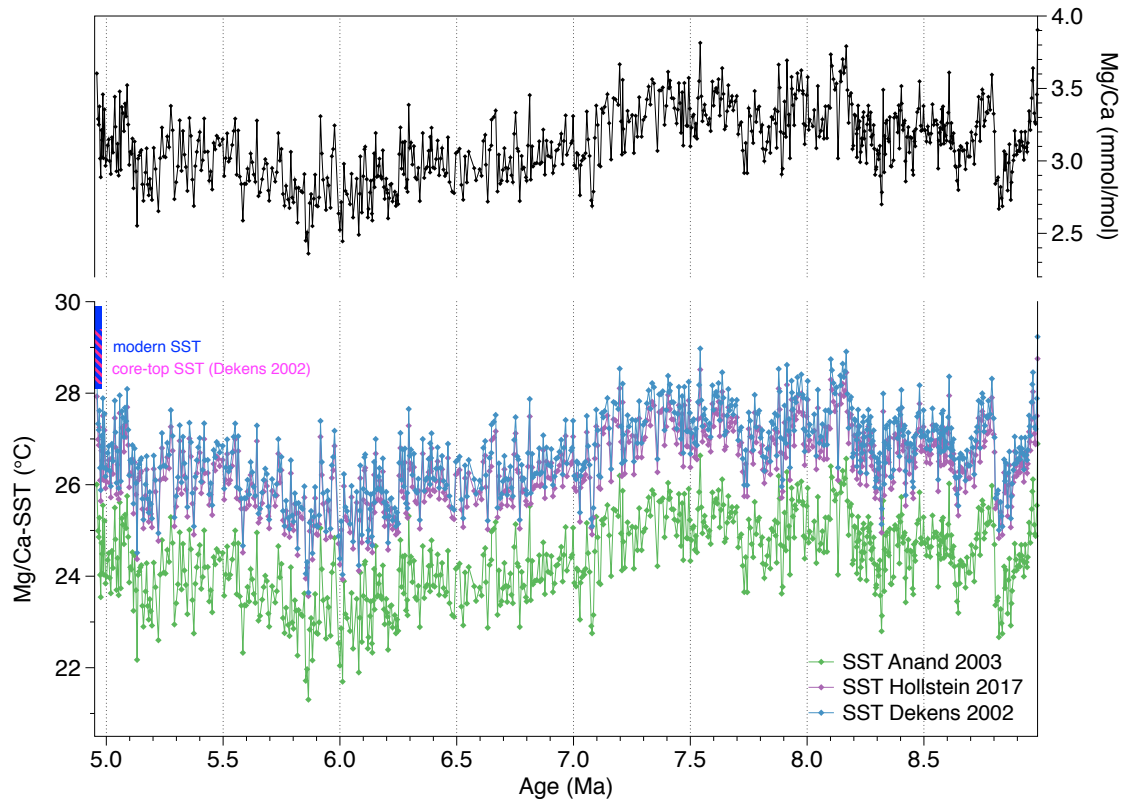


90

91

92 **Figure S2. Sensitivity test of Mg/Ca ratio to foraminifera test size.**

93  $\Delta\text{Mg}/\text{Ca}$ , calculated as the Mg/Ca ratio (mmol/mol) of the 212- 315  $\mu\text{m}$  size fraction minus the  
94 Mg/Ca ratio (mmol/mol) of the 355- 500  $\mu\text{m}$  size fraction, plotted against temperature calculated  
95 for the 212-315  $\mu\text{m}$  size fraction using the Anand et al. (2003) calibration equation.



96  
97  
98  
99  
100  
101  
102  
103  
104

**Figure S3. Effect of application of different Mg/Ca-T calibrations on reconstructed SSTs.**

Black curve: Mg/Ca ratio measured in *T. trilobus* tests, blue curve: SST calculated with the calibration of Dekens et al (2002), green curve: SST calculated with the calibration of Anand et al. (2003), purple curve: SST calculated with the calibration of Hollstein et al. (2017). The SST range from Site U1443 core-top Mg/Ca data is calculated with the calibration of Dekens et al. (2002).

105 **Text S3. Scenarios for Late Miocene Mg/Ca<sub>sw</sub> reconstruction**

106  
107  
108  
109  
110  
111  
112  
113  
114  
115

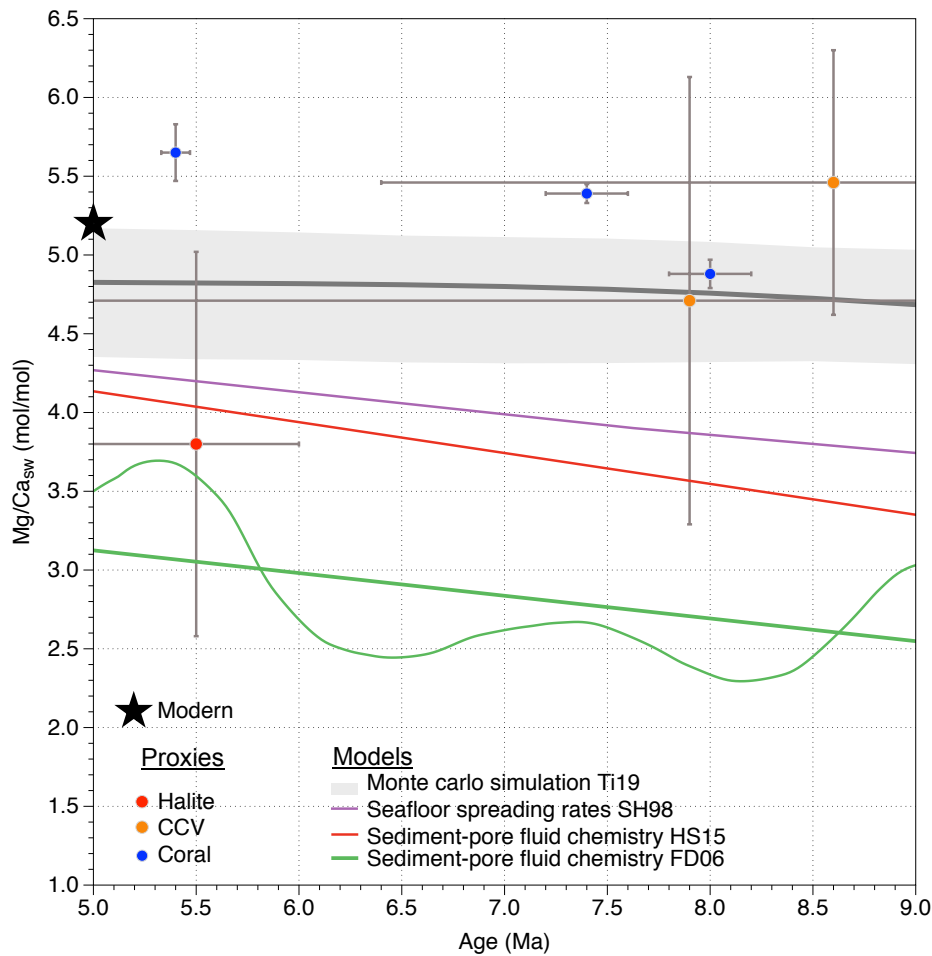
In the history of the Phanerozoic ocean, changes in weathering input by rivers, hydrothermal activity, and carbonate deposition have led to changes in Mg and Ca concentration of seawater. The variation in Mg/Ca of seawater (Mg/Ca<sub>sw</sub>) can in turn affect Mg/Ca ratio in foraminiferal tests (Mg/Ca<sub>test</sub>) precipitated in this seawater. Therefore, for studies longer than ~1 Ma (residence time of Ca; Broecker & Peng, 1982) it is important to correct Mg/Ca<sub>test</sub> for Mg/Ca<sub>sw</sub> variations to accurately reconstruct Mg/Ca derived temperature. For example, previous studies (Medina-Elizalde et al., 2008; O'Brien et al., 2014) have demonstrated the importance of adjusting Mg/Ca-SST to Mg/Ca<sub>sw</sub> variations for understanding past climate dynamics and sensitivity.

116  
117  
118  
119  
120  
121

Because past proxy reconstructions of Mg/Ca<sub>sw</sub> have low temporal resolution, wide errors bars and are not always in good agreement with each other, Mg/Ca<sub>sw</sub> reconstruction requires modeling studies. Among many existing scenarios (Berner 2004; Demicco et al., 2005; Fantle & DePaolo, 2006; Farkas et al., 2007; Higgins & Schrag, 2012; Stanley & Hardie, 1998, Wilkinson & Algeo, 1989) we selected three scenarios in agreement with Mg/Ca<sub>sw</sub> reconstruction derived from proxies and fitting their error bars. The SH98 scenario (Stanley & Hardie 1998) is a model based on

122 seafloor spreading rate and scenarios FD06 (Fantle & DePaolo, 2006) and HS15 (Higgins &  
 123 Schrag, 2015) are derived from chemical modelling of pore fluids and carbonate sediments (Mg,  
 124 Ca and Sr) in the Ontong-Java Plateau (ODP Leg 130 Site 807). Works of Higgins & Schrag  
 125 (2012 and 2015) follow the work of Fantle & DePaolo (2006), but they provide new constraints  
 126 on the diagenetic effect on pore fluid chemistry. They use Mg isotopic profiles of sediment and  
 127 pore fluid to determine the partition coefficient of Mg in recrystallized calcite allowing them to  
 128 determine how much of Mg in pore fluid is due to recrystallization (and not linked to Mg/Ca<sub>sw</sub>  
 129 variation). Because the original FD06 scenario implies some unrealistic short-term Mg/Ca<sub>sw</sub>  
 130 variations given the residence time of Mg and Ca in the ocean, in Figure S4 a simple linear  
 131 relationship was applied. Therefore, the HS15 scenario is our preferred scenario, but we compare  
 132 the effect of the three scenarios (and the effect of H value) on reconstructed SST in the Figure S5.  
 133

134 In Figure S4, we also included the Mg/Ca<sub>sw</sub> Monte Carlo simulation from Tierney et al. (2019)  
 135 based on available proxy data (grey line and grey shading). This simulation includes data from  
 136 corals (Gothmann et al., 2015), leading to considerable variability in terms of Mg/Ca<sub>sw</sub> estimates.  
 137 Given that the controls on Mg incorporation in modern corals are complex and not fully  
 138 understood, we did not use this proposed Mg/Ca<sub>sw</sub> reconstruction in our study.  
 139  
 140



141 **Figure S4. Mg/Ca<sub>sw</sub> scenarios for the late Miocene (9-5 Ma).**  
 142 Scenario SH98 in purple (Stanley & Hardie, 1998), scenario HS15 in red (Higgins & Schrag,  
 143 2015) and scenario FD06 in green (Fantle & DePaolo, 2006). For scenario FD06 a simple linear  
 144

145 relation was applied instead of the initial scenario. Mg/Ca<sub>sw</sub> data are from halite fluid inclusions  
146 (Horita et al., 2001), fossil corals (Gothmann et al., 2015) and calcium carbonate veins (CCV;  
147 Coggon et al., 2010). The Monte Carlo simulation is from Tierney et al. (2019) and is based on  
148 proxy data. The modern Mg/Ca<sub>sw</sub> of 5.2 mol/mol is indicated by the star.

149  
150

151 **Text S4. Effect of Mg/Ca<sub>sw</sub> correction and relation between Mg/Ca<sub>sw</sub> and Mg/Ca<sub>test</sub> on**  
152 **reconstructed SST**

153

154 There is no agreement in the literature concerning the Mg/Ca<sub>sw</sub>-Mg/Ca<sub>test</sub> relation and whether it is  
155 a power law (Evans & Muller, 2012) or linear (Tierney et al., 2019) relation.

156 The work of Evans & Muller (2012) suggested that the incorporation of Mg into calcite varies  
157 non-linearly with Mg/Ca<sub>sw</sub>, necessitating a power law to correct Mg/Ca<sub>test</sub> for Mg/Ca<sub>sw</sub> variations  
158 in the following form:

159 
$$Mg/Ca_{test} = \frac{F \times Mg/Ca_{sw}^{t=tH}}{F \times Mg/Ca_{sw}^{t=0H}} \times Bexp^{AT}$$

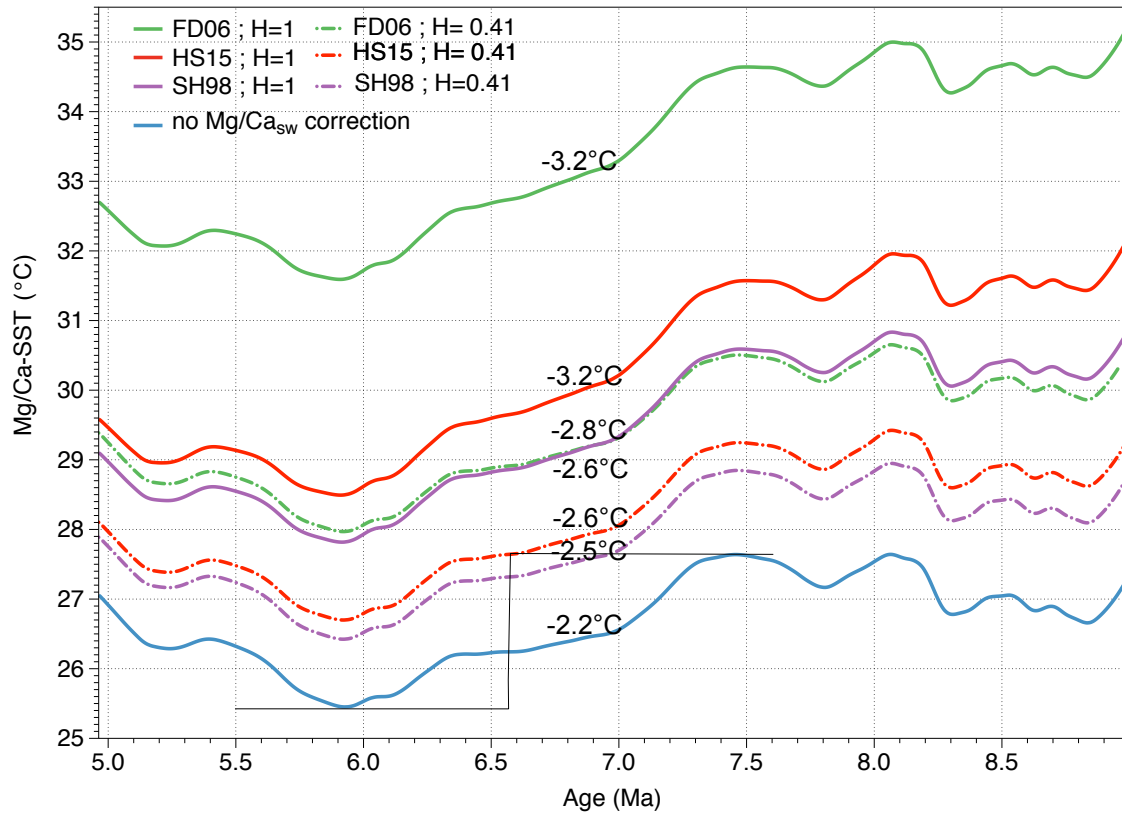
160

161 With F and H being species-specific constants (for *T. sacculifer* H=0.41; data based on culture  
162 experiment from Delaney et al., 1985) and modern Mg/Ca<sub>sw</sub> = 5.2 mol/mol (Broecker & Peng,  
163 1982). On the other hand, Tierney et al. (2019) found a H value close to 1 for many species of  
164 foraminifera including *T. sacculifer* (data also based on culture experiment from Delaney et al.,  
165 1985), and suggested that a simple linear relation more adequately defines the Mg/Ca<sub>sw</sub>- Mg/Ca<sub>test</sub>  
166 relation. We also note that the study of Evans et al. (2016) proposed that the temperature  
167 sensitivity of Mg/Ca in foraminifera changes with Mg/Ca<sub>sw</sub> but this effect has only been detected  
168 in culture experiment on one species of planktic foraminifera, *Globigerinoides ruber*, and was not  
169 reported in studies of benthic foraminiferal species (De Nooijer et al., 2017).

170

171 In order to have a global view on the possible range of absolute SST and amplitude of long term  
172 cooling associated with Mg/Ca<sub>sw</sub> correction and H value, a comparison is made in Figure S5.  
173 Mg/Ca<sub>sw</sub> corrections increase absolute temperature and amplitude of long term variation of  
174 reconstructed SST compared to uncorrected Mg/Ca<sub>sw</sub>-SST. With no correction for Mg/Ca<sub>sw</sub> the  
175 long term gradual cooling recorded from 7.4 to 5.8 Ma is 2.2 °C (Figure S5, blue curve), for  
176 HS15 scenario with a linear relation between Mg/Ca<sub>sw</sub> and Mg/Ca<sub>test</sub> it is 3.2 °C and with a power  
177 law relationship and H value of 0.41 it is 2.6 °C (Figure S5, red curve and red dashed curve). As  
178 works of Evans & Muller (2012) and Tierney et al. (2019) are based on the same data derived  
179 from the *T. sacculifer* culture experiment from Delaney et al., (1985), we prefer to use the linear  
180 relationship in our study as it provides a more simplistic approach, but further culture experiments  
181 are needed to better constrain how Mg incorporates into calcite tests of *T. sacculifer* at varying  
182 Mg/Ca<sub>sw</sub>. The two most extreme scenarios are scenario FD06 H=1 with SST values comprised  
183 between 35 and 32 °C and a long-term cooling of 3.2 °C (Figure S5 green curve), and scenario  
184 SH98 H=0.41 with SST values comprised between 29 and 26 °C and a long-term cooling of 2.5  
185 °C (Figure S5 purple dashed curve). Our preferred scenario HS15 H=1 is in red, SST values are  
186 comprised between 32 and 29 °C and the amplitude of long term cooling is 3.2 °C.

187

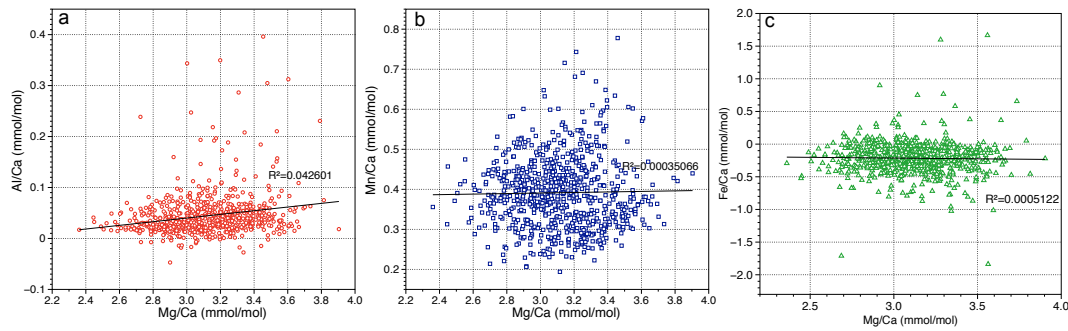


188  
 189  
 190  
 191  
 192  
 193  
 194  
 195  
 196  
 197  
 198

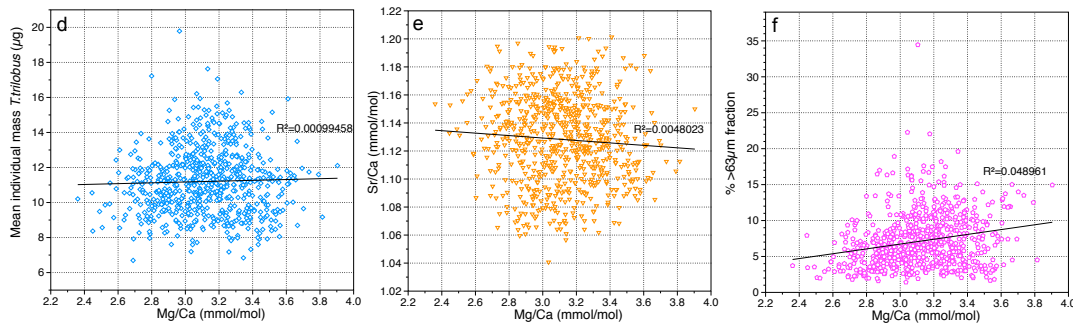
**Figure S5. Effect of scenarios SH98, FD06 and HS15, and H value on absolute SST reconstruction and amplitude of variations.**

For clarity only the long term SST trend is shown (calculated with a 10 % Lowess filter). Mg/Ca-SSTs were calculated using the Dekens et al. (2002) *T. sacculifer* calibration equation for the Pacific, without correction for Mg/Ca<sub>sw</sub> (blue curve) and corrected for Mg/Ca<sub>sw</sub> variability following HS15 scenario (red curves), FD06 scenario (green curves) and SH98 scenario (purple curves), with linear relation (solid lines) and power law relation with H=0.41 for *T. sacculifer* (dashed lines).

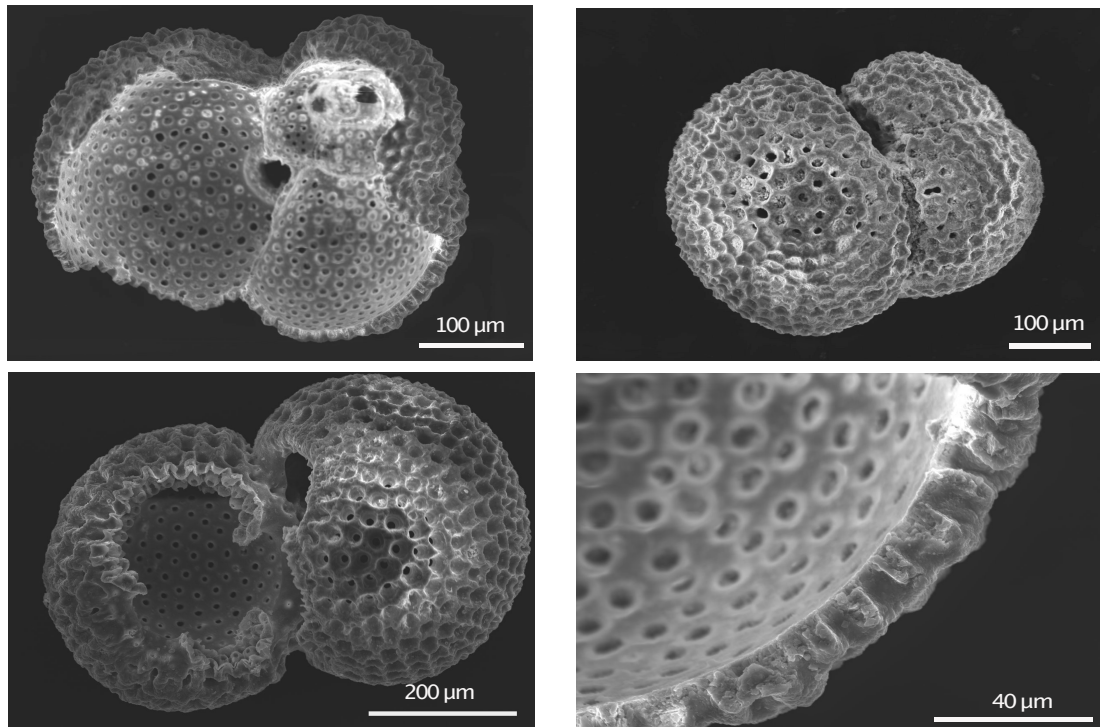
### Contamination indices



### Dissolution indices



199



200

201

### Figure S6. Contamination and dissolution indices and SEM images.

202

Contamination indices: (a) Al/Ca, (b) Mn/Ca, (c) Fe/Ca (mmol/mol), and dissolution indices: (d)

203

mean individual mass of *T. trilobus* ( $\mu\text{g}$ ) (e) Sr/Ca (mmol/mol) and (f) % >63  $\mu\text{m}$  coarse fraction

204

showing no significant correlation with Mg/Ca (mmol/mol), suggesting that Mg originates from

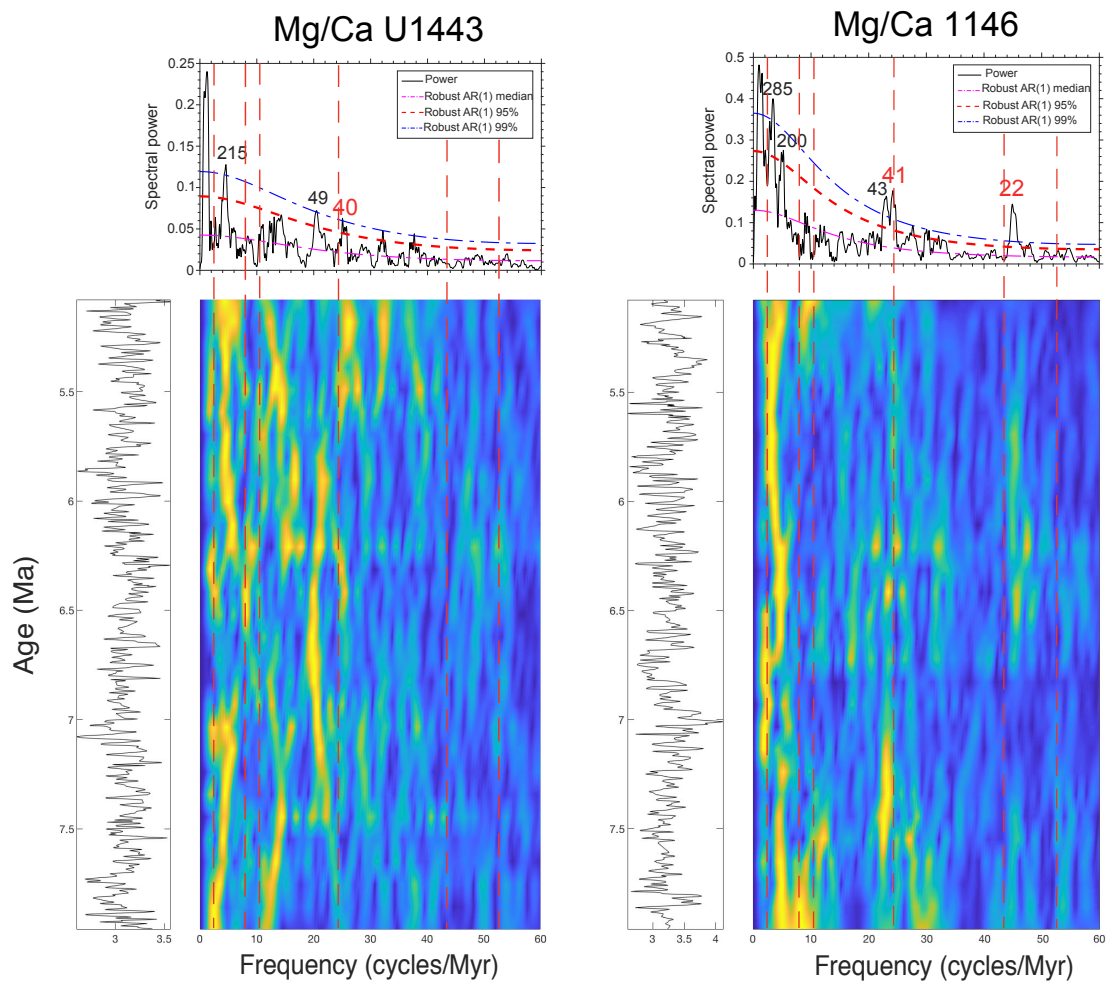
205

foraminiferal tests and not from mineral contamination and that dissolution is not driving the

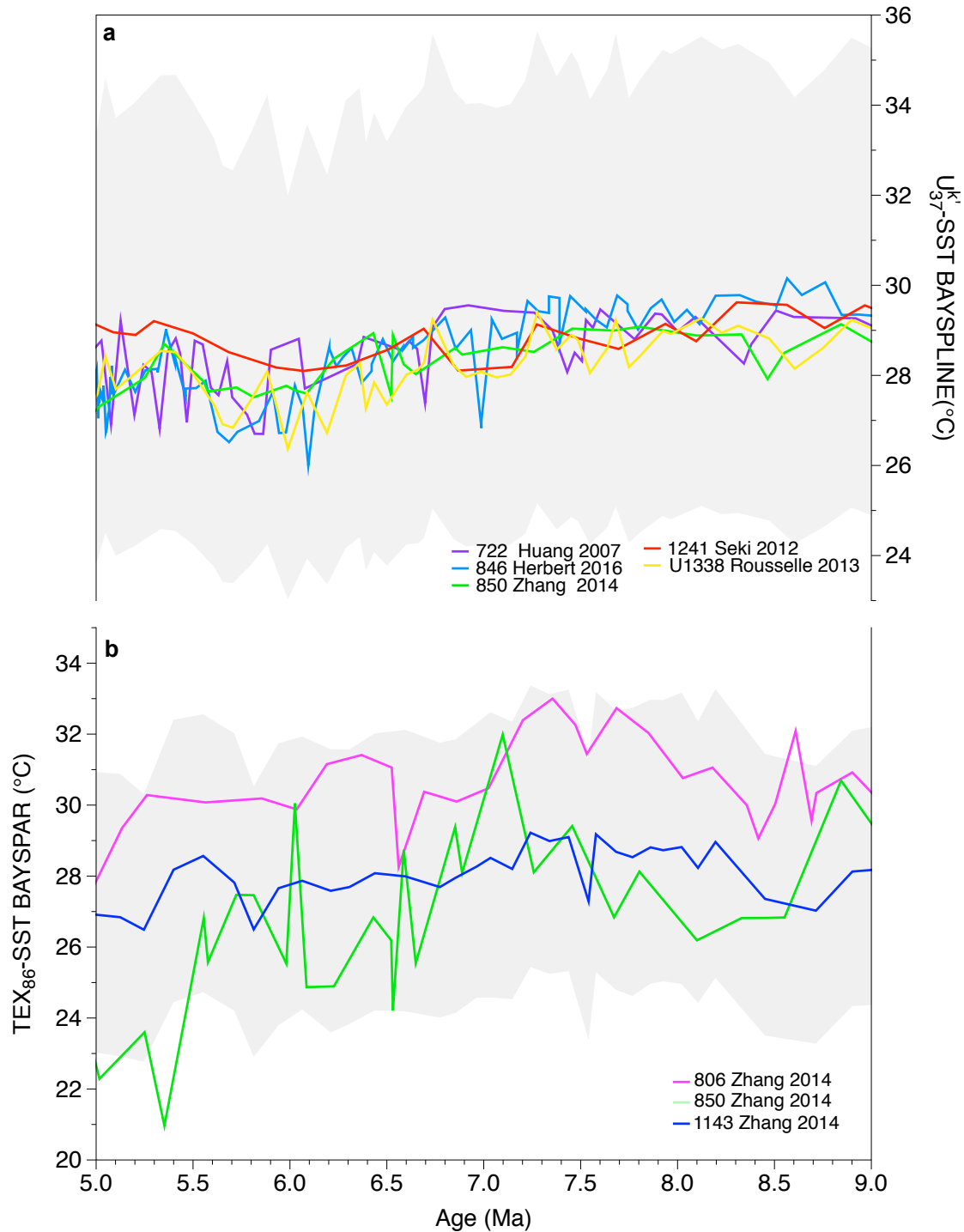
206

Mg/Ca trend. Scanning Electron Microscopy (SEM) images of *T. trilobus* tests showing a good

207 apparent preservation of tests (inner and external walls, cross-section of wall and pore structure)  
 208 and minor effect of diagenesis.  
 209

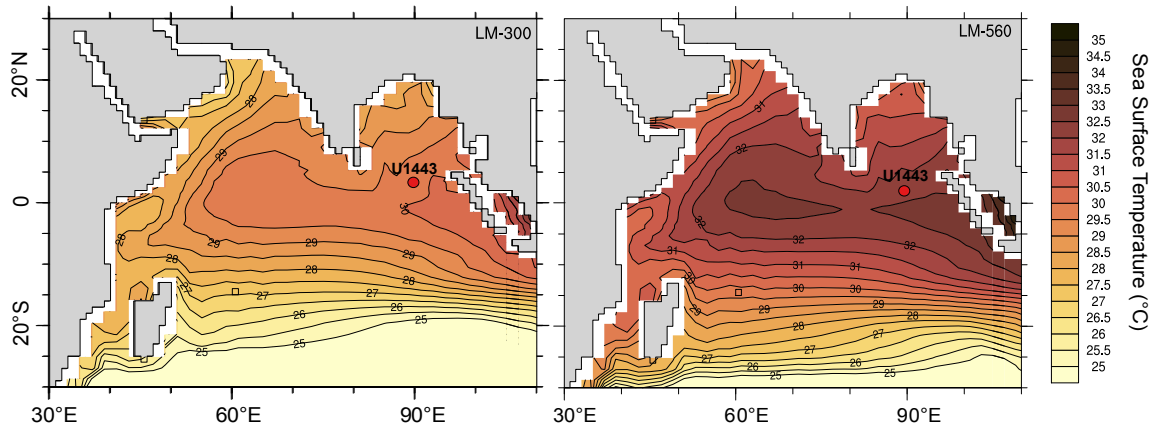


210  
 211  
 212 **Figure S7. Time series analyses of Mg/Ca from Site U1443 (South Bay of Bengal) and Site**  
 213 **1146 (South China Sea).**  
 214 Spectral analysis (Multi Taper Method, MTM) and evolutive spectral analysis (Fast Fourier  
 215 Transform, LAH) (see Methods), left: Mg/Ca at Site U1443 in Southern Bay of Bengal, right:  
 216 Mg/Ca at Site 1146 in South China Sea (Holbourn et al., 2018). For the two data sets MTM (top)  
 217 and LAH (right) are performed on filtered records (left) (see Methods). Primary periods are in red  
 218 and heterodynes are in black, red dotted line indicate periods of 404, 124, 95, 41, 24, 22 and 19  
 219 kyr resulting from Earth's orbital periods. Sampling resolution is similar in Site U1443 and Site  
 220 1146 indicating that the absence of significant power in the precession band after ~8 Ma and the  
 221 lower power in the obliquity band at Site U1443 compared to Site 1146 are real features and are  
 222 not an artifact of lower sampling resolution.



223  
 224  
 225  
 226  
 227  
 228  
 229  
 230  
 231

**Figure S8. Tropical low resolution temperature records based on  $U_{37}^K$  and  $TEX_{86}$  indices.** (a) Tropical  $U_{37}^K$  SST records recalculated using the BAYSPLINE calibration (Tierney & Tingley, 2018). For clarity the  $1.5\sigma$  uncertainty estimate is only shown for one record (U1338); all records have a similar amplitude error envelope due to similar estimated SSTs. (b) Tropical  $TEX_{86}$  SST records recalculated using the BAYSPAR calibration Analog mode (Tierney & Tingley, 2015).



232  
 233  
 234  
 235  
 236  
 237  
 238  
 239

**Figure S9. The effect of  $p\text{CO}_2$  variations on modelled SSTs in the intertropical Indian Ocean during the late Miocene.**

Right: Modelled SSTs with late Miocene boundary conditions and 2X preindustrial  $p\text{CO}_2$  (560 ppm), representing condition at ~8 Ma. Left: Modelled SSTs with late Miocene boundary condition and  $p\text{CO}_2$  concentrations at 300 ppm, representing conditions at ~6 Ma. In the two maps the paleolocation of Site U1443 at 6 and 8 Ma is shown (left and right, respectively).